

Theoretical Analysis of Cooperative Driving at Idealized Unsignalized Intersections

Shen Li, Jiawei Zhang, Zhenwu Chen*, and Li Li*

Abstract: Cooperative driving is widely viewed as a promising method to better utilize limited road resources and alleviate traffic congestion. In recent years, several cooperative driving approaches for idealized traffic scenarios (i.e., uniform vehicle arrivals, lengths, and speeds) have been proposed. However, theoretical analyses and comparisons of these approaches are lacking. In this study, we propose a unified group-by-group zipper-style movement model to describe different approaches synthetically and evaluate their performance. We derive the maximum throughput for cooperative driving plans of idealized unsignalized intersections and discuss how to minimize the delay of vehicles. The obtained conclusions shed light on future cooperative driving studies.

Key words: cooperative driving; connected and automated vehicles; unsignalized intersection

1 Introduction

Connected and Automated Vehicles (CAVs) are expected to revolutionize road traffic because we can collect useful information via vehicle-to-everything (V2X) communication and plan their movements to fully utilize limited road resources. If we can successfully implement cooperative driving in practice, then we will undoubtedly improve traffic safety and efficiency^[1–4].

In the past decade, various studies of cooperative driving have been conducted. Several studies focused on how to establish reliable V2X communication for cooperative driving^[5, 6]. Some studies emphasized the self-organized controller design of individual vehicles^[7]. Other studies discussed how to formulate a good

cooperative driving plan for multiple vehicles, so that these vehicles can pass a certain conflict point (e.g., unsignalized intersection, ramp areas, and working zones) as quickly as possible. In this study, we also address this issue.

Generally, cooperative driving planning can be roughly categorized into two kinds, namely, studies of non-idealized traffic scenarios^[8–11] and studies of idealized traffic scenarios. In the first kind of study, researchers assume that the vehicles' lengths, arrivals, driving directions, and speeds are all random and time-varying^[12–14]. Under such assumptions, we need to design adaptive and intelligent planning algorithms to schedule a short-term feasible passing order for the investigated vehicles, so that their delay can be minimized. Here a possible passing order for vehicles refers to an assignment of the right-of-way of vehicles for the critical conflict point^[15–18].

In the second kind of study, researchers assume that the vehicles' lengths, arrivals, driving directions, and speeds are all uniform. Under such assumptions, we aim to design a long-term cooperative driving plan to maximize the possible throughput or minimize the delay in a relatively long period. In such studies, the influence of all of the other factors was neglected to highlight the dominant impact of passing orders. Then, the key

• Shen Li is with the Department of Civil Engineering, Tsinghua University, Beijing 100084, China. E-mail: sli299@tsinghua.edu.cn.

• Jiawei Zhang and Li Li are with the Department of Automation, Tsinghua University, Beijing 100084, China. E-mail: zhangjw20@mails.tsinghua.edu.cn; li-li@tsinghua.edu.cn.

• Zhenwu Chen is with the Shenzhen Urban Transport Planning Center Co., Ltd., Shenzhen 518000, China. E-mail: czw@sutpc.com.

* To whom correspondence should be addressed.

Manuscript received: 2022-09-08; revised: 2022-11-09; accepted: 2022-12-29

problem becomes which long-term cooperative driving plan generates the best passing order^[19, 20].

One typical example of cooperative driving for idealized traffic scenarios is the rhythmic control method proposed in Refs. [21, 22]. This method aims to enable vehicles to pass through an intersection in a conflict-free manner with a preset rhythm. More precisely, vehicles running in different directions are assumed to sequentially take the right-of-way via a one-by-one zipper-style movement. Thus, a certain gap must be retained between every two consecutive vehicles running in the same lane and let a certain vehicle that moves in the other direction run across this gap. Notably, the proposed rhythmic control considerably increases the intersection capacity.

Another typical example of cooperative driving for idealized traffic scenarios is the modular vehicle method proposed in Refs. [21, 23]. Modular vehicles originally referred to vehicles whose capacity can be flexibly changed during operations. That is, a vehicle can be composed of an indefinite number of Modular Units (MUs) to dynamically vary its capacity by concatenating or detaching MUs across different dispatches. In several studies, researchers used modular vehicle techniques to arrange a certain number of vehicles to pass the intersection as a seamless vehicle queue. Compared with conventional platoon-based intersection control^[24–27], modular vehicles can further condense traffic flow, thus improving traffic throughput.

However, no synthetic study to compare various cooperative driving approaches for idealized traffic scenarios, particularly unsignalized intersection scenarios, has been conducted. The parameters of several driving plans that were manually designed cannot be easily generalized to other scenarios. Several important questions remained to be answered:

First, is there any simple yet intuitive explanation for the efficiency of rhythmic control? Is there any theory for determining the parameters of rhythmic control?

Second, can we combine modular vehicles and rhythmic control? Are these two approaches completely contradicting each other?

In this study, we proposed a unified group-by-group zipper-style movement model to analyze idealized cooperative driving synthetically and evaluate their performance fairly. We assume that vehicle groups driving in different directions will sequentially take the right-of-way of a certain conflict point via a one-

by-one zipper-style movement. When the group size degenerates to one, we obtain the one-by-one zipper-style movement model or the equivalent rhythmic control. When the group size increases to some large numbers, we achieve fixed-time signal control with the modular vehicle method. Through the unified group-by-group zipper-style movement model, we determine that these two extreme solutions can be appropriately combined. In other words, rhythmic control and fixed-time signal control with modular vehicles are exactly the two sides of one coin.

In ideal situations, the time gap between two consecutive vehicles in the same group can be kept to zero, and the time gap between any two adjacent groups in different driving directions can be kept to the lowest value (or even zero when necessary). Thus, the time resource of a conflict point can be maximally utilized.

Different from dynamic cooperative driving plans for non-idealized traffic scenarios, the periodic/cyclic nature of unified group-by-group zipper-style plans has some interesting and clear conclusions. First, we theoretically determine the upper bound of the throughput for a simple two-way intersection. We determine that, in many situations (e.g., when the inflow rates of different lanes of an unsignalized intersection are uneven), rhythmic control may not be the best cooperative driving plan because the strict one-by-one zipper-style movements may lead to a waste of time resource. By contrast, our unified model can help reach the maximum throughput with a better arrangement of group sizes. Then, we discuss how to achieve the shortest delay of vehicles when the throughput requirement is satisfied. We observe that the smaller the group size is, the shorter the delay. Thus, rhythmic control might be the best choice if it could satisfy the throughput requirement. Otherwise, we propose an algorithm to determine the best group size. Finally, we explain how to extend the obtained conclusions to build a more complex cooperative driving plan for complex intersections with multiple lanes.

To provide a clear explanation of our findings, the remainder of this paper is organized as follows: In Section 2, we briefly review several related studies. In Section 3, we introduce a unified model to analyze different cooperative driving approaches for the simplest idealized unsignalized intersection scenarios. In Section 4, we generalize the conclusions obtained in Section 3 to other idealized traffic scenarios. Finally, in Section 5, we conclude the paper.

2 Literature Review

With the aid of V2X communication, CAVs can share their driving states (i.e., position, velocity, and acceleration) and intentions to cooperatively coordinate their movements when passing conflict points. Specifically, researchers began to show interest in complex cooperative driving around unsignalized intersections in the mid-2000s^[8, 9], where vehicles were allowed to drive in various directions.

Several related studies aim to reach an appropriate driving plan by directly solving the detailed trajectories of every individual vehicle^[19]. Usually, we will formulate a mathematical programming problem in which the decision variables are the discretized trajectories of every vehicle. Suppose we use a certain number of midway points sampled at certain time points to represent a trajectory. Then, we can describe the time/energy-optimal and the collision-free/lane-keeping conditions with the constraints among the coordinates of these midway points^[28]. By solving the obtained mathematical programming problems, we can derive an appropriate cooperative driving plan^[29]. However, these programming problems are often difficult to solve because they usually contain integer variables that indicate whether one vehicle will pass the conflict point before the other vehicle.

By contrast, many other studies first determine the passing orders of vehicles and then calculate the corresponding trajectories of vehicles. Dresner and Stone^[9] first proposed the reservation-based method or first come, first served mechanism. In the approaches reported in Refs. [30–34], the vehicle sends a conflict point access request to the control center based on their possible arrival time. If the intersection space required for that arrival time is unoccupied, then the request is granted; conversely, the vehicle slows down and resubmits a new request. In terms of request priority, the vehicle that enters the control area earlier has a higher priority to apply. The calculation complexity of such approaches is low, but the obtained cooperative driving plan is often far inferior to the optimal cooperative driving plan.

Li and Wang^[8] were the first to investigate planning-based passing order selection. Various planning methods have been employed to represent and search the solution spaces spanned by all of the possible passing orders. One frequently used planning method is to construct a search tree containing all feasible crossing sequences,

where each node of the search tree corresponds to a feasible solution^[12, 13]. The original tree node pruning algorithm can guarantee that the optimal cooperative driving plan is identified; however, it is time-consuming when the number of vehicles is large^[8]. The recently proposed Monte Carlo tree search algorithm can help in identifying a good enough cooperative driving plan within a short time budget^[17].

The aforementioned cooperative driving approaches assumed random and time-varying vehicles' arrivals and driving directions. Thus, we need to provide flexible driving plans to maximize the throughput and minimize the delay. Implementing such driving plans requires complicated vehicle movements and intensive V2X communication.

By contrast, some recent studies assumed regular vehicles' arrivals and driving directions to build simplified cooperative driving plans. Such plans are based on the hidden relationship between conflict points and time slot formulations of cooperative driving plans for isolated intersections^[31, 33, 35, 36]. To guarantee that vehicles will not collide with each other at the conflict points, we can equivalently require them to occupy a special conflict point one-by-one. If we further require that vehicles of different flows occupy a special conflict point in a locally sequential yet globally periodic manner, then we can obtain another interesting time slot interpretation of the cooperative driving plan. In other words, for each conflict point, we can preset a certain number of time slots along the time axis and let vehicles from different flows occupy this conflict point cyclically^[20, 37].

Different design methods for such preset cyclic cooperative driving plans have been employed. One typical example is the rhythmic control method proposed in Refs. [22, 38], as illustrated in Fig. 1a. Such a method considered a complex symmetric intersection with three lanes, where Lanes 1, 2, and 3 of each leg are through, through, and left-turn lanes, respectively. Then, a complex preset time slot assignment plan was designed to ensure that every two consecutive vehicles moving in the same direction will be right separated by a vehicle moving in another direction at a certain conflict point. Such design is delicate and places every issue in a highly correlated composition. The parameters of the proposed design are manually selected and not well explained. Therefore, theoretical analyses to examine whether rhythmic control considerably increases the intersection capacity are lacking.

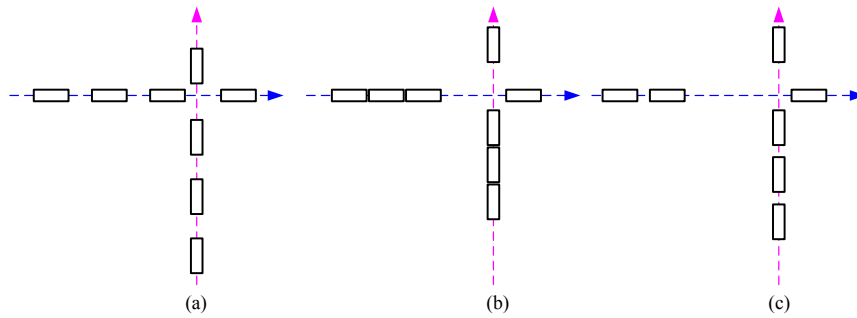


Fig. 1 Illustration of different control methods at the simplest conflict point, where vehicles run in only two directions: (a) rhythmic control, where vehicles pass with the one-by-one zipper-style movement; (b) modular vehicles control, where vehicles condense the car-following gap or even diminish such gap to increase the intersection capacity; (c) platoon-based control, where vehicles in the same direction are grouped to pass the intersection, but there is a gap between vehicles in the same group.

Rhythmic control utilizes the gap between every two consecutive vehicles moving in the same direction by letting a different-way vehicle run through this gap. A typical question is whether we can further condense this gap or even diminish such gap to increase the intersection capacity. The modular vehicle method proposed in Refs. [23, 38] is a typical example that follows this idea. The modular vehicle method arranges a certain number of vehicles to pass the intersection as a seamless vehicle queue. Different from conventional platoon-based intersection control^[39, 40], the modular vehicle method ideally assumes that there are no gaps between vehicles so that we can save that recourse to accommodate more vehicles to increase the intersection capacity, as illustrated in Figs. 1b and 1c.

However, most of the current modular vehicle studies emphasize the network-wide transport arrangement problems. Whether the modular vehicle method can be an alternative or combined with the rhythmic control method remains to be answered.

3 Simplest Idealized Unsignalized Intersection

3.1 Group-by-group zipper-style cooperative driving

We take the simple intersection, which only has two-direction flows (or streams in the classical traffic signal control context), e.g., west-to-east and south-to-north flows, as a basic example. Each lag of this intersection has only one lane; thus, we have only one conflict point in such scenarios. We will explain other cases that can be generalized from this simple case in Section 4. Without losing generality, we assume that all of the vehicles are running at the maximum possible speed v and the lengths of all vehicles are the same L . These assumptions are

common in idealized cooperative driving studies.

In this study, we set up a group-by-group zipper-style movement of vehicles, as illustrated in Fig. 2a. In other words, a group of vehicles in the west-to-east flow will pass the intersection right after a group of vehicles in the south-to-north flow that passes the intersection, and vice versa, cyclically. Without losing generality, we assume that the first group of vehicles in the west-to-east flow passes the core area before the first group of vehicles in the south-to-north flow passes the core area. Let us set the original time point as the starting time point of an hour.

Suppose we divide the west-to-east flow into several groups of vehicles. Each group has k_1 vehicles. The south-to-north flow is also divided into several groups of vehicles. Each group has k_2 vehicles. Such a division strategy assumes uniform vehicle arrivals. When $k_1 = k_2 = 1$, the movement plan degenerates to the one-by-one zipper-style movement, which is equivalent to rhythmic control proposed in Refs. [22, 38]. When k_1 and k_2 are large enough, the movement plan degenerates to the ordinary fixed-time signal control^[26, 41–43].

We assume that the time gap between every two consecutive vehicles in a group for the west-to-east flow is set to a constant value Δt_1 . The time gap between every two consecutive vehicles in a group for the south-to-north flow is set to a constant value Δt_2 . As discussed in Refs. [44, 45], we define the time gap as the time difference between the rear bumper of the leading vehicle and the front bumper of the following vehicle. Δt_1 and Δt_2 are introduced to model the necessary safe distance between vehicles that prevent rear-end collisions. Notably, the achieved minimum time gap is 0.6 s for AV platoons under some special Cooperative Adaptive Cruise Control (CACC) driving conditions^[46]. If we can reach the ideal $\Delta t_1 = \Delta t_2 = 0$,

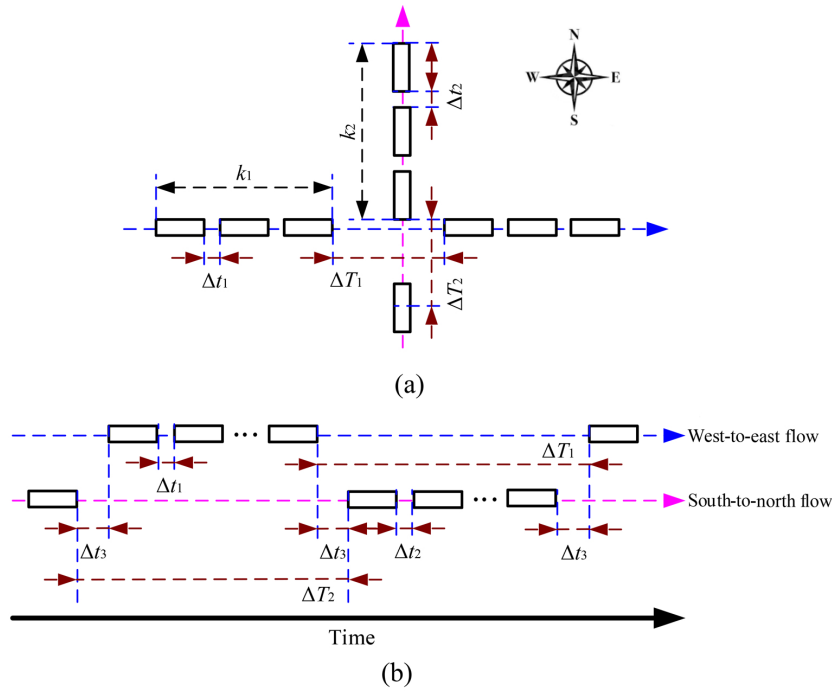


Fig. 2 (a) Illustration of cooperative driving at the simplest conflict point, where vehicles run in only two directions; (b) the corresponding right-of-way assignments for the conflict point illustrated using the virtual vehicle mapping technique.

then the movement plan degenerates into the modular autonomous vehicles proposed in Refs. [21, 23].

We can adopt the virtual vehicle mapping technique proposed in Refs. [47, 48] to map the vehicles moving in the south-to-north flow to the west-to-east flow. Then, we can obtain the corresponding right-of-way assignments for the conflict point along the time axis for the two flows shown in Fig. 2b. The original time point is the time that the first group of vehicles in Lane 1 passes the conflict point between Lanes 1 and 2. The time value for every vehicle in Lane 1 or 2 indicates its arrival time to the conflict point.

Here, we set the time gap between every two consecutive groups of vehicles in the west-to-east flow as ΔT_1 and the time gap between every two consecutive groups of vehicles in the south-to-north flow as ΔT_2 . Suppose the time gap between the first vehicle of a group of vehicles in the west-to-east flow and the last vehicle of the succeeding group of vehicles in the south-to-north flow is set as Δt_3 . Similarly, the time gap between the first vehicle of a group of vehicles in the south-to-north flow and the last vehicle of the succeeding group of vehicles in the west-to-east flow is set as Δt_3 . Notably, Δt_3 is introduced to model the necessary safe distance between vehicles that prevent side collisions.

We determine that a group of vehicles in the west-to-east flow pass the intersection between two consecutive

groups of vehicles in the south-to-north flow and vice versa, cyclically. By observing the occupying sequence of the conflict point along the time axis, we derive the following expressions:

$$(k_1 - 1) \Delta t_1 + k_1 \frac{L}{v} + 2\Delta t_3 \leq \Delta T_2 \quad (1)$$

$$(k_2 - 1) \Delta t_2 + k_2 \frac{L}{v} + 2\Delta t_3 \leq \Delta T_1 \quad (2)$$

We further assume the upstream inflow rate of the west-to-east flow is q_1 veh/h and the inflow rate of the south-to-north flow is q_2 veh/h. The vehicles coming from upstream are originally uniformly distributed and will be appropriately guided to form some condensed groups before they enter the core area of the unsignalized intersection. Such assumptions are widely adopted for idealized cooperative driving^[13, 17] (see Fig. 3 for an illustration). Our focus is on the passing orders within the core area, and the movements in the adjusting area are not addressed in idealized cooperative driving studies. For presentation simplicity, we assume that, in 1 h, m_1 groups of vehicles of the west-to-east flow pass through the core area and m_2 groups of vehicles of the south-to-north flow pass through the core area. Thus, we either have $m_1 = m_2$ or $m_1 = m_2 + 1$ because we assume that the first group of vehicles in the west-to-east flow passes first. Because of the round-off effect, it could be possible that not all of the k_1 or k_2 vehicles of the last

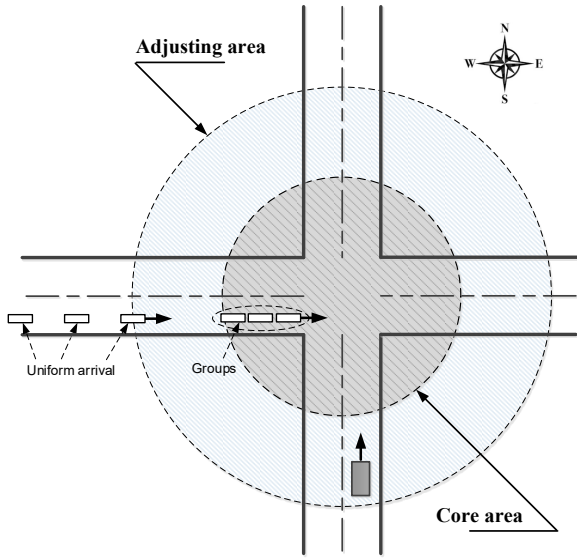


Fig. 3 Illustration of the condensing process before cooperative driving at the core area of an unsignalized intersection.

group can pass the core area within the 1 h threshold. However, such round-off errors can be negligible when q_1 and q_2 are large.

3.2 Throughputs of different cooperative driving plans

In idealized cooperative driving studies, we usually assume that L and v are preselected constants. We are interested in two related problems:

Problem 1 Given the upstream inflow rates q_1 and q_2 , determine a cooperative driving plan that is characterized by a 9-tuple (i.e., $k_1, k_2, \Delta t_1, \Delta t_2, \Delta t_3, \Delta T_1, \Delta T_2, m_1$, and m_2) to “serve” such inflow rates. Here, “serve” means to make all of the vehicles pass through the core area with a bounded non-increasing delay. If the vehicles are jammed outside the core area and the lengths of the jammed queues increase with time, then we say that the cooperative driving plan cannot “serve” such inflow rates.

Problem 2 Determine the maximum upstream inflow rates $q_1 + q_2$ that can be served by a given cooperative driving plan that is characterized by a 9-tuple (i.e., $k_1, k_2, \Delta t_1, \Delta t_2, \Delta t_3, \Delta T_1, \Delta T_2, m_1$, and m_2). Based on the previously drawn conclusions, we can compare the performance of different cooperative driving methods.

Let us investigate the first problem. Suppose a cooperative driving plan can “serve” the upstream inflow rates q_1 and q_2 . Thus, we should approximately dispatch all q_1 vehicles in the west-to-east flow in 1 h (3600 s) as follows:

$$m_1 k_1 \geq q_1 \quad (3)$$

$$q_1 \left(\Delta t_1 + \frac{L}{v} \right) + m_2 \Delta T_1 \leq 3600 \quad (4)$$

Similarly, we should approximately dispatch all q_2 vehicles in the south-to-north flow in 1 h (3600 s) as follows:

$$m_2 k_2 \geq q_2 \quad (5)$$

$$q_2 \left(\Delta t_2 + \frac{L}{v} \right) + m_1 \Delta T_4 \leq 3600 \quad (6)$$

Notably, we do not require $m_1 k_1 = q_1$ and $m_2 k_2 = q_2$. As discussed in Refs. [31, 33, 35], such group-by-group zipper-style movements of vehicles define a series of time slots along the time axis. Formulas (3) and (5) guarantee that we have reserved enough time slots for the coming vehicles. If no vehicle arrives in time for a time slot, then we just leave this preset time slot (or the corresponding position in the groups of the west-to-east and/or south-to-north flows) unoccupied.

We draw the following conclusions:

Theorem 1 A cooperative driving plan (i.e., $k_1, k_2, \Delta t_1, \Delta t_2, \Delta t_3, \Delta T_1, \Delta T_2, m_1$, and m_2) can “serve” the upstream inflow rates q_1 and q_2 if they satisfy the Formulas (1) – (6).

Theorem 1 seems a bit tricky, but we can analyze several special cases to obtain some useful insights.

Theorem 2 Rhythmic control proposed in Refs. [22, 38] is a cooperative driving plan ($k_1 = k_2 = 1, \Delta t_1$, and Δt_2 are not involved; $\Delta t_3 = 0, \Delta T_1 = \Delta T_2, m_1 = m_2$). Rhythmic control can “serve” the upstream inflow rates q_1 and q_2 if

$$\frac{L}{v} \leq \frac{1800}{\max \{q_1, q_2\}} \quad (7)$$

Proof From Formulas (1) and (2), we derive the following expression:

$$\frac{L}{v} \leq \Delta T_1 = \Delta T_2 \quad (8)$$

From Formulas (3) and (5), we derive the following expression:

$$m_1 = m_2 = \max \{q_1, q_2\} \quad (9)$$

By combining Formulas (4), (6), (8), and (9), we derive the following expression:

$$\max \{q_1, q_2\} \frac{L}{v} + \max \{q_1, q_2\} \Delta T_1 \leq 3600 \quad (10)$$

which can satisfy Formulas (4) and (6). Thus, we achieve a sufficient condition (i.e., Formula (11)) for the service problem by selecting the time gaps between two consecutive groups of vehicles running in the same

direction, as follows:

$$\frac{L}{v} \leq \Delta T_1 = \Delta T_2 = \frac{1800}{\max\{q_1, q_2\}} \quad (11)$$

This concludes the proof for Formula (7). ■

The rhythmic control method proposed in Refs. [22, 38] requires a strictly symmetric one-by-one zipper-style movement, thereby wasting some road resources. Indeed, we can relax the constraints and obtain an asymmetric group-by-group zipper-style movement to better “serve” the imbalanced inflow rates q_1 and q_2 . Without losing generality, we assume that $q_1 > q_2$.

Theorem 3 The asymmetric cooperative driving plan (i.e., $k_1, k_2, \Delta t_1 = \Delta t_2 = \Delta t_3 = 0, \Delta T_1, \Delta T_2, m_1$, and m_2) can “serve” the upstream inflow rates q_1 and q_2 if

$$\frac{L}{v} \leq \frac{3600}{q_1 + q_2} \quad (12)$$

Proof From Formulas (1) and (2), we derive the following expression:

$$k_2 \frac{L}{v} \leq \Delta T_1 \quad (13)$$

From Formulas (3) and (5), we derive the following expression:

$$m_1 k_1 \geq q_1 > (m_1 - 1)k_1 \quad (14)$$

By combining Formulas (4), (6), (13), and (14), we achieve a sufficient condition for Formula (12) using the following expression:

$$\Delta T_1 = k_2 \frac{L}{v}, \Delta T_2 = \frac{3600 - m_2 \Delta T_1}{m_2 + 1}, k_1 = \left\lfloor \frac{\Delta T_1 v}{L} \right\rfloor \quad (15)$$

to conclude this proof. Here, the function $\lfloor \cdot \rfloor$ is the integer flooring function. ■

Notably, the asymmetric cooperative driving plan can “serve” the imbalanced inflow rates and, whereas the rhythmic control proposed in Refs. [22, 38] cannot do so.

We also regard this cooperative driving plan (i.e., $k_1, k_2, \Delta t_1 = \Delta t_2 = \Delta t_3 = 0, \Delta T_1, \Delta T_2, m_1$, and m_2) as a fixed-time signal control plan with modular vehicle techniques. Given certain appropriate k_1 and k_2 , we can set the green-phase time for the west-to-east flow as $\Delta T_1 \approx 3600k_2 / (q_1 + q_2)$ and the green-phase time for the south-to-north flow as $\Delta T_2 \approx 3600k_1 / (q_1 + q_2)$. The throughput of the intersection will be the same if we use this fixed-time signal control plan. Thus, we easily draw the following conclusion:

Theorem 4 For the simple intersection discussed in this section, the maximum upstream inflow rate $q_1 + q_2$ that can be served by a given cooperative driving plan

is the same as that served by the best fixed-time signal control plan. In other words, we derive the following upper bound:

$$\max\{q_1 + q_2\} = 3600 \frac{L}{v} \quad (16)$$

We determine that the rhythmic control method proposed in Refs. [22, 38] uses the vehicles in a different direction to split the vehicles in the same direction. If we set $\Delta t_1 = \Delta t_2 > 2\Delta t_3 + \frac{L}{v}$ for some applications, then the rhythmic control method may yield more throughput than the fixed-time signal control plan. The numerical example provided in Refs. [22, 38] fits such conditions.

3.3 Delay of vehicles and feasible cooperative driving plan search algorithm

The previously presented analysis indicates that we can have different cooperative driving plans that “serve” the same inflow rates q_1 and q_2 but the resulting delays for vehicles in different flows can vary significantly. Let us consider an extreme example: we have $q_1 \gg 1$ vehicles of the west-to-east flow and $q_2 = 1$ vehicles of the south-to-north flow. Cooperative driving vehicle plan *A* first dispatches q_1 vehicles of the west-to-east flow to pass the core area and then dispatches only one vehicle of the south-to-north flow (i.e., we set $k_1 = q_1$ and $k_2 = 1$). Cooperative driving vehicle plan *B* dispatches the first $q_2/2$ vehicles of the west-to-east flow to pass the core area, then dispatches only one vehicle of the south-to-north flow, and finally dispatches the first $q_1/2$ vehicles of the west-to-east flow (i.e., we set $k_1 = q_1$ and $k_2 = 1$). We determine that the maximum delays of the south-to-north flow obtained by the two plans are quite different.

To retain the equity of different travelers, we need to distribute the benefits and costs to travelers fairly and appropriately^[49–52]. Thus, we are interested in the following problem:

Problem 3 Suppose the upstream inflow rates q_1 and q_2 can be served by a certain number of cooperative driving plans. Determine the plan that provides the lowest maximum delay for vehicles.

Suppose a cooperative driving plan that is characterized by a 9-tuple (i.e., $k_1, k_2, \Delta t_1, \Delta t_2, \Delta t_3, \Delta T_1, \Delta T_2, m_1$, and m_2) can “serve” the upstream inflow rates q_1 and q_2 . We assume uniform arrival of vehicles. Without any delay, the i -th vehicle of the west-to-east flow should arrive at the core area at time

$$t_{\text{ideal}}^i = \frac{3600}{q_1} i \quad (17)$$

When the cooperative driving plan is applied, the i -th vehicle of the west-to-east flow should arrive at the core area at time

$$t_{\text{real}}^i = \left\lceil \frac{i-1}{k_1} \right\rceil \left[(k_1-1) \Delta t_1 + k_1 \frac{L}{v} + 2\Delta t_3 + \Delta T_1 \right] + [(i \bmod k_1) - 2]^+ \Delta t_1 + [(i \bmod k_1) - 1] \frac{L}{v} \quad (18)$$

where function $(M \bmod N)$ yields the remainder of M divided by N ; function $[x]^+ = \max\{0, x\}$.

The delay of the i -th vehicle of the west-to-east flow can then be written as follows:

$$t_{\text{delay}}^i = [t_{\text{real}}^i - t_{\text{ideal}}^i]^+ \quad (19)$$

Similarly, we determine the delay of the j -th vehicle of the south-to-north flow and formulate our decision problem as follows:

$$\begin{aligned} & \min_{k_1, k_2 \in N} \max_{i \in \{1, 2, \dots, q_1\}, j \in \{1, 2, \dots, q_2\}} \{t^i, t^j\} \\ & \text{s.t., Formulas (1)–(6) and Eqs. (17)–(19)} \end{aligned} \quad (20)$$

The programming problem expressed in Formula (20) is difficult to solve because of the complicated round-off operations of integer decision variables. However, we can derive a simple upper bound for the maximum delay.

Theorem 5 The upper bound for the maximum delay of any vehicle is derived as follows:

$$\Delta T_1 + \Delta T_2 \quad (21)$$

If we can further apply an asymmetric cooperative driving plan (i.e., $k_1, k_2, \Delta t_1 = \Delta t_2 = \Delta t_3 = 0, \Delta T_1, \Delta T_2, m_1$, and m_2), then we should select the minimum $\Delta T_1 + \Delta T_2$.

Proof Based on Formula (14), we derive $m_1 k_1 = q_1$ for the west-to-east flow. Thus, the i -th vehicle of the west-to-east flow should arrive at the core area at time

$$t_{\text{ideal}}^i = \frac{3600}{q_1} i = \frac{3600}{m_1 k_1} i \quad (22)$$

Considering the periodic feature of the cooperative driving plans, we roughly derive the following expression:

$$m_1 \left\{ k_1 \frac{L}{v} + \Delta T_1 \right\} = 3600 \quad (23)$$

By combining Eqs. (22) and (23), we derive the following expression:

$$t_{\text{ideal}}^i = \frac{\frac{L}{v} + \Delta T_1}{k_1} i \quad (24)$$

Further considering Eq. (18) and Formula (1), we derive the following expression:

$$t_{\text{delay}}^i = [t_{\text{real}}^i - t_{\text{ideal}}^i]^+ \leq \Delta T_1 + \Delta T_2 \quad (25)$$

Such a condition also holds for the delay t_{delay}^j of the j -th vehicle of the south-to-north flow. This concludes the proof. ■

Further considering Formula (11), we derive the following expression:

$$(k_1 + k_2) \frac{L}{v} \leq \Delta T_1 + \Delta T_2 \quad (26)$$

Based on Eq. (22) and Formula (25), we select the smallest possible k_1 and k_2 that “serve” the inflow rates q_1 and q_2 to reduce the lowest maximum delay of every individual vehicle. This indicates that when the condition in Formula (7) is satisfied, the rhythmic control method leads to the lowest maximum delay and is suggested. However, when the condition in Formula (7) is not satisfied, but the condition in Formula (11) is satisfied, we should select the following cooperative driving plan.

Because we aim to keep k_1 and k_2 as small as possible, given q_1 and q_2 , we can identify the ideal asymmetric cooperative driving plan using Algorithm 1 assuming $\Delta t_1 = \Delta t_2 = \Delta t_3 = 0$.

Theorem 4 guarantees that we can finally obtain a satisfactory solution if Formula (12) holds. Let us use a simple test case to illustrate the algorithm. Suppose $L/v = 1$ s, $q_1 = 2100$ veh/h, and $q_2 = 1000$ veh/h. The rhythmic control method cannot “serve” such inflow rates. When $k_2 = 1$, we obtain $\Delta T_1 = 1$ s, $m_2 = 1000$, $\Delta T_2 \approx 2.6$ s, $k_1 = 2$, and $m_1 = 1001$. At that point, we derive $m_1 k_1 < q_1$. Thus, we increment $k - 2$ to $k_2 = 2$. We obtain $\Delta T_1 = 2$ s, $m_2 = 500$, $\Delta T_2 \approx 5.19$ s, $k_1 = 5$, $m_1 = 501$, and $m_1 k_1 > q_1$. This cooperative driving plan can “serve” such inflow rates. Indeed, such a cooperative driving plan (i.e., $k_1 = 5, k_2 = 2, \Delta t_1 = \Delta t_2 = \Delta t_3 = 0, \Delta T_1 = 5.19, \Delta T_2 = 1, m_1 = 501$, and $m_2 = 500$) can at most “serve” the upstream inflow rates $q_1 = 2500$ veh/h and $q_2 = 1000$ veh/h. If this plan is applied to the upstream inflow rates $q_1 = 2100$ veh/h and $q_2 = 1000$ veh/h, then some positions in the groups of the west-to-east flow (or the equivalent planned time slots^[31, 33, 35, 36]) will be left unoccupied.

4 From Simple Intersections to Complex Intersections

In this section, we will show how to gradually add

Algorithm 1 Search for a feasible cooperative driving plan

Step 0: Set $k_2 = 1$

Step 1: Let $\Delta T_1 = k_2 \frac{L}{v}$, $m_2 = \left\lceil \frac{q_2}{k_2} \right\rceil$, $\Delta T_2 = \frac{3600 - m_2 \Delta T_1}{m_2 + 1}$,

$k_1 = \left\lceil \frac{\Delta T_1 v}{L} \right\rceil$, $m_1 = m_2 + 1$. Here, the function $\lceil \cdot \rceil$ is the integer ceiling function.

Step 2: If $m_1 k_1 \geq q_1$, then exit the algorithm; otherwise, set $k_2 = k_2 + 1$ and go to Step 2 for another round of scans.

more lanes to the simplest two-lane intersection to build more complex driving scenarios. The previously drawn conclusions can be easily extended to new cases.

4.1 Adjacent and nonadjacent lanes

Let us first consider the three-lane intersection shown in Fig. 4, which has two west-to-east flow lanes (i.e., Lanes 1 and 3) and one south-to-north flow lane (i.e., Lane 2). The two west-to-east flow lanes are adjacent to each other. We can assume that the upstream inflow rates for Lanes 1 and 3 are the same in such cases because no left-right turns are considered. Suppose we determine the cooperative driving plan for Lanes 1 and 2 as what has been explained previously without considering Lane 3. We can copy the cooperative driving plan for Lane 1 as the cooperative driving plan for Lane 3, expecting to enlarge the safety gap Δt_3 for all of the lanes to avoid side collisions. We did not consider the time lag between Lanes 1 and 3 because they are adjacent in space. We can aggregate such lanes and consider them as a whole as a special flow (stream) without causing problems.

Let us then consider the other three-lane intersection shown in Fig. 5a, which has one west-to-east flow lane (i.e., Lane 1), one east-to-west flow lane (i.e., Lane 3), and one south-to-north flow lane (i.e., Lane 2). Different from that shown in Fig. 4, we assume a non-negligible space distance $\mu_{1,3}$ between Lanes 1 and 3. Without losing generality, we assume that the upstream inflow rate of Lane 3 is q_3 and $q_3 < q_1$. Thus, the west-to-east flow in Lane 1 is the mainstream in this case. First, we can determine the cooperative driving plan for Lanes 1 and 2, as explained previously, without considering Lane 3.

Then, we can copy the cooperative driving plan for Lane 1 as the cooperative driving plan for Lane 3, further considering a phase time lag $\varphi_{1,3}$ between two lanes to allow a group of vehicles in Lane 2 to run across Lanes 1 and 3 sequentially without any interruption. Thus, we obtain the right-of-way assignments along the time axis, as shown in Fig. 5b. The original time point is the

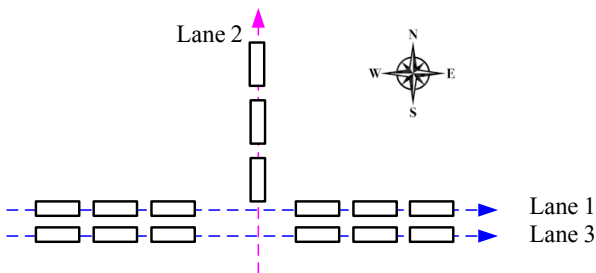


Fig. 4 Three-lane intersection with two west-to-east flow lanes and one south-to-north flow lane.

time that the first group of vehicles in Lane 1 passes the conflict point between Lanes 1 and 2. The time value for every vehicle in Lane 1 or 2 indicates its arrival time to the conflict point between Lanes 1 and 2. The time value for every vehicle in Lane 3 indicates its arrival time to the conflict point between Lanes 2 and 3.

Let us still assume that the first group of vehicles in Lane 1 will pass the conflict point between Lanes 1 and 2 before the first group of vehicles in Lane 2. Thus, the first group of vehicles in Lane 2 will arrive at the conflict point between Lanes 2 and 3 at time $\Delta T_2 + \mu_{1,3}/v$. We assume that the first group of vehicles in Lane 3 has just passed the conflict point between Lanes 2 and 3. As shown in Fig. 5b, the phase time lag $\varphi_{1,3}$ between the west-to-east flow in Lane 1 and the east-to-west flow in Lane 3 could be expressed as follows:

$$\varphi_{1,3} = \Delta T_2 + \mu_{1,3}/v - \Delta T_1 = \mu_{1,3}/v \quad (27)$$

In other words, the i -th group of vehicles in Lane 3 will arrive at the conflict point between Lanes 2 and 3 with a phase time lag $\mu_{1,3}/v$ to the time that the i -th group of vehicles in Lane 1 arrives at the conflict point between Lanes 1 and 2. The obtained cooperative driving plans for the three lanes can ensure that every vehicle

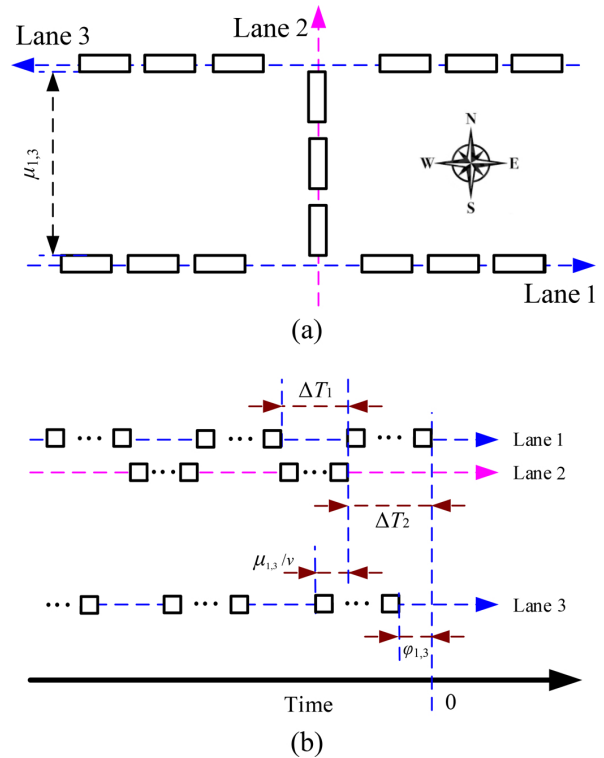


Fig. 5 Three-lane intersection with different flow lanes and the right-of-way assignments along the time axis. (a) Three-lane intersection with one west-to-east flow lane, one east-to-west flow lane, and one south-to-north flow lane; (b) the corresponding right-of-way assignments along the time axis.

uninterruptedly passes the core area with speed v if the upstream inflow rates can be served.

Notably, in many urban roads, the left-most lane of one flow is adjacent to the left-most lane of the opposite flow. Under such conditions, no time lag exists between opposite flows. The corresponding cooperative driving plan degenerates to fixed-time signal control with modular vehicle technique. The method applied in Section 3 can be easily extended to design the driving plan and analyze the throughput/delay of vehicles.

4.2 Mirror-symmetric cooperative driving for intersections with only through lanes

Indeed, we can view cooperative driving plans for idealized unsignalized intersections as special fixed-time signal timing plans assuming that (1) all vehicles move with constant speed within the core area of the intersection, (2) the gaps between any two consecutive vehicles are minimized to nearly zero, and (3) the green time for a certain flow can be short (e.g., < 1 s for rhythmic control).

We focus on mirror-symmetric cooperative driving plans in this study. Here, mirror symmetry means that the cooperative driving plans for opposite flows are the same, except for certain time lags. The rhythmic control method is a typical kind of mirror-symmetric cooperative driving plan. Mirror-symmetric cooperative driving plans introduce more constraints to the design; therefore, their maximum throughputs may be lower than some asymmetric alternative plans. The maximum throughput of a mirror-symmetric plan should be determined using the flows with the largest upstream inflow rates.

Let us consider a four-lane intersection labeled as counterclockwise, as shown in Fig. 6a, which has one west-to-east flow lane (i.e., Lane 1), one east-to-north flow lane (i.e., Lane 3), one south-to-north flow lane (i.e., Lane 2), and one north-to-south flow lane (i.e., Lane 4). We assume that non-negligible space distances exist between every two parallel lanes. Without losing generality, we assume that the upstream inflow rate of Lane 3 is q_3 and $q_3 < q_1$ and the upstream inflow rate of Lane 4 is q_4 and $q_4 < q_2$. Thus, the west-to-east flow in Lane 1 and the south-to-north flow lane in Lane 2 are the mainstreams in this case. First, we determine the cooperative driving plan for Lanes 1 and 2, as explained previously, without considering Lanes 3 and 4. Then, we copy the cooperative driving plan for Lane 1 as the cooperative driving plan for Lane 3 and copy the cooperative driving plan for Lane 2 as the cooperative

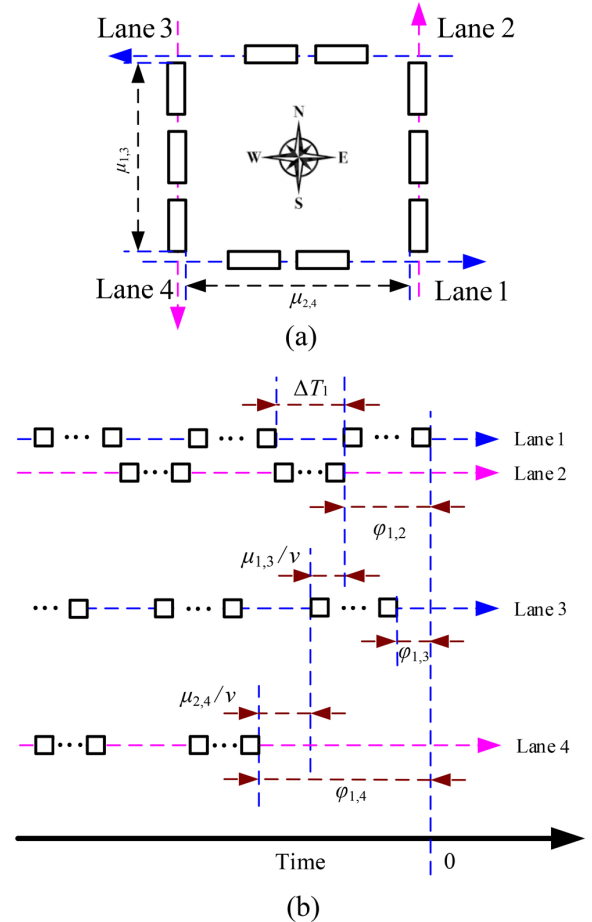


Fig. 6 Four-lane intersection with different flow lanes and the right-of-way assignments along the time axis. (a) Four-lane intersection with lanes labeled as counterclockwise; (b) the corresponding right-of-way assignments along the time axis.

driving plan for Lane 4, except for introducing some phase time lags.

As shown in Fig. 6b, the original time point is set as the time that the first group of vehicles in Lane 1 passes the conflict point between Lanes 1 and 2. The time value for every vehicle in Lane 1 or 2 indicates its arrival time to the conflict point between Lanes 1 and 2. The time value for every vehicle in Lane 3 indicates its arrival time to the conflict point between Lanes 2 and 3. The time value for every vehicle in Lane 4 indicates its arrival time to the conflict point between Lanes 3 and 4. The phase time lags between Lane 1 and the other lanes are defined as $\varphi_{1,2}$, $\varphi_{1,3}$, and $\varphi_{1,4}$. That is, the p -th group of vehicles in Lane 4 will arrive at the conflict point between Lanes 3 and 4 with a phase time lag $\varphi_{1,4}$ to the time that the p -th group of vehicles in Lane 1 arrives at the conflict point between Lanes 1 and 2. Indeed, we set $\varphi_{1,2} = \Delta T_2$ directly in all of the previously presented

discussions. Let us still adopt $\varphi_{1,3} = \mu_{1,3}/v$.

From Fig. 6b, we can set the following expression:

$$\varphi_{1,4} = \varphi_{1,2} + \varphi_{1,3} + \mu_{2,4}/v \quad (28)$$

Thus, the first group of vehicles in Lane 4 will arrive at the conflict point between Lanes 4 and 1 at time

$$\varphi_{1,4} + \mu_{1,3}/v = \Delta T_2 + \mu_{2,4}/v + 2\mu_{1,3}/v \quad (29)$$

If the first group of vehicles in Lane 4 catches up with the end of the second group of vehicles in Lane 1 when arriving at the conflict point between Lanes 4 and lane 1, then an ouroboros pattern will be generated, which can be expressed as follows:

$$\begin{aligned} \varphi_{1,4} + \mu_{1,3}/v = \Delta T_2 + \mu_{2,4}/v + 2\mu_{1,3}/v = \\ 2\Delta T_2 + \Delta T_1 - \mu_{2,4}/v \end{aligned} \quad (30)$$

or equivalently

$$2\mu_{2,4}/v + 2\mu_{1,3}/v = \Delta T_2 + \Delta T_1 \quad (31)$$

If the aforementioned constraints hold, then we can ensure that every vehicle uninterruptedly passes the core area with speed v under the mirror-symmetric cooperative driving plan. Specifically, for the one-by-one zipper-style movement, which is equivalent to rhythmic control, we derive $\mu_{1,3} = \mu_{2,4} = \mu$ and $\Delta T_1 = \Delta T_2 = L/v$. Based on Eq. (31), we derive $\varphi_{1,2} = \varphi_{1,3} = L/v$ and $\varphi_{1,4} = (3L)/(2v)$, with the following road geometry requirement:

$$\mu = pL/2 \quad (32)$$

If the intersection is an ordinary intersection where all opposite lanes are adjacent, then we obtain $\mu_{1,3} = \mu_{2,4} = 0$. Thus, $\varphi_{1,3} = 0$ and $\varphi_{1,2} = \varphi_{1,4} = \Delta T_2$, which naturally degenerate a two-phase fixed-time signal timing plan with the modular vehicle technique.

4.3 Cooperative driving for complex intersections

Let us consider an eight-lane intersection labeled as counterclockwise, as shown in Fig. 7, which has one west-to-east flow lane (i.e., Lane 1), one east-to-north flow lane (i.e., Lane 3), one north-to-south flow lane (i.e., Lane 2), one south-to-north flow lane (i.e., Lane 4), one east-to-north flow lane (i.e., Lane 5), one south-to-west flow lane (i.e., Lane 6), one east-to-south flow lane (i.e., Lane 7), and one north-to-east flow lane (i.e., Lane 8).

The design difficulty lies in the left-turn flows. For example, Lane 5 sequentially intersects with Lanes 4, 6, 8, and 3. The appropriate cooperative driving plan is difficult to calculate when the group size of vehicles is not one. Generally, two ways are employed to solve this problem.

The first way is to allow the vehicles of left-turn flows to pass the intersection nonsynchronously. Moreover,

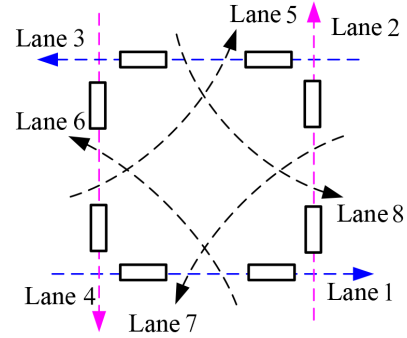


Fig. 7 Eight-lane intersection with four through lanes first labeled as counterclockwise and four left-turn lanes then labeled as counterclockwise.

the vehicles of left-turn flows will not share the same period as the vehicles of through flows. For the lane intersection shown in Fig. 7, we set a two-phase period for the vehicles of left-turn flows. In the first phase, at some appropriate time slots, we let a few vehicles in Lanes 5 and 7 enter the core area without causing queue spillover and dispatch them when possible. We can always enlarge ΔT_1 and ΔT_2 to reserve enough time slots allowing left-turn vehicles to pass the conflict points between the through and left-turn lanes. Then, in the second phase, we dispatch a few vehicles in Lanes 6 and 8.

The most valuable merit of the first way is its simplicity. Because we do not need to consider the interactions between vehicles in different left-turn lanes, we can simply change the cooperative driving plan obtained in Section 4.2 to realize it. Furthermore, we can still handle imbalanced upstream inflow rates because the group size of vehicles in different lanes can be larger than 1 and asymmetric.

The second way is to adopt the one-by-one zipper-style movement, which is equivalent to the rhythmic control method. We can carefully set up the distances between neighboring conflict points and the speed of vehicles to enable vehicles to pass each conflict point in a delicate head-to-tail connecting manner. Because exceptional examples have been provided in Refs. [22, 38], we will not further discuss the intricate calculations here.

The previously presented analysis indicates that for some intersections allowing complex vehicle-moving directions, we can gradually build cooperative driving plans, just like putting construction bricks together to build castles. When we set the group size of all lanes to be one, we can also obtain the cooperative driving plans proposed in rhythmic control^[22, 38] or erasing

lane control^[20]. This bottom-up establishing process can explain how we can achieve delicate rhythmic control like the cooperative driving plan originally presented through an up-bottom manner in Refs. [22, 38].

The subtle interlaced time lag assignment introduced in rhythmic control places extra limits on the intersection capacity, particularly when we meet strictly imbalanced upstream inflow rates. Thus, different cooperative driving plans can be appropriately modified based on the change in upstream inflow rates.

5 Conclusion

In this study, we provide a unified group-by-group zipper-style movement model to combine the rhythmic control and modular vehicle methods that have been proposed for cooperative driving at idealized unsignalized intersections. When the group size degenerates to one, we utilize the rhythmic control method. When the group size increases to a large number, we employ fixed-time signal control with the modular vehicle method. This trick enables us to integrate two different cooperative driving plans together and reveal the essence of some showy cooperative driving plans.

Different from existing approaches, our model theoretically analyzes the throughput/delay of vehicles and reveals the key difference between different cooperative driving methods. We show that our new model may outperform existing approaches when we meet significantly imbalanced upstream inflow rates. The obtained conclusions set a basis for further analysis of cooperative driving methods, particularly on the adaptive planning-based cooperative driving method^[12–14, 28, 29, 53], which had not been theoretically investigated.

This study focuses on the maximum throughput and minimum delay for idealized situations. When applied in practice, we cannot assume the safety gap $\Delta t_1 = \Delta t_2 = \Delta t_3 = 0$. How to select the safety distances Δt_1 , Δt_2 , and Δt_3 to balance traffic efficiency and safety remains challenging. Specifically, when we consider mixed traffic flow in which CAVs and human-driven vehicles share roads^[39, 40, 54–57], we might dynamically maintain different safety distances when following CAVs and human-driven vehicles. We hope more researchers will show interest in this interesting research direction. We believe the combination of classical signal timing design skills and recently developed cooperative driving methods can lead to more interesting results.

Acknowledgment

This work was supported by the National Natural Science Foundation of China (No. 52272420), the Science and Technology Innovation Committee of Shenzhen (No. CJGJZD20200617102801005), and the Tsinghua-Toyota Joint Research Institution.

References

- [1] L. Li, D. Wen, and D. Y. Yao, A survey of traffic control with vehicular communications, *IEEE Trans. Intell. Transport. Syst.*, vol. 15, no. 1, pp. 425–432, 2014.
- [2] Q. Guo, L. Li, and X. Ban, Urban traffic signal control with connected and automated vehicles: A survey, *Transp. Res. Part C: Emerg. Technol.*, vol. 101, pp. 313–334, 2019.
- [3] J. Zhang, C. Chang, H. Pei, X. Peng, Y. Guo, R. Lian, Z. Chen, and L. Li, CAVSim: A microscope traffic simulator for connected and automated vehicles environment, in *Proc. 2022 IEEE 25th Int. Conf. Intelligent Transportation Systems (ITSC)*, Macau, China, 2022, pp. 3719–3724.
- [4] C. Chang, K. Zhang, J. Zhang, S. Li, and L. Li, Driving safety monitoring and warning for connected and automated vehicles via edge computing, in *Proc. of the 2022 IEEE 25th Int. Conf. Intelligent Transportation Systems (ITSC)*, Macau, China, 2022, pp. 3940–3947.
- [5] S. Chen, J. Hu, Y. Shi, L. Zhao, and W. Li, A vision of C-V2X: Technologies, field testing, and challenges with Chinese development, *IEEE Internet of Things J.*, vol. 7, no. 5, pp. 3872–3881, 2020.
- [6] H. Zhou, W. Xu, J. Chen, and W. Wang, Evolutionary V2X technologies toward the internet of vehicles: Challenges and opportunities, in *Proc. IEEE*, vol. 108, no. 2, pp. 308–323, 2020.
- [7] J. Zhang, C. Chang, X. Zeng, and L. Li, Multi-agent DRL-based lane change with right-of-way collaboration awareness, *IEEE Trans. Intell. Transport. Syst.*, vol. 24, no. 1, pp. 854–869, 2023.
- [8] L. Li and F. Y. Wang, Cooperative driving at blind crossings using intervehicle communication, *IEEE Trans. Veh. Technol.*, vol. 55, no. 6, pp. 1712–1724, 2006.
- [9] K. Dresner and P. Stone, A multiagent approach to autonomous intersection management, *J. Artif. Intell. Res.*, vol. 31, no. 1, pp. 591–656, 2008.
- [10] Y. Meng, L. Li, F. Y. Wang, K. Li, and Z. Li, Analysis of cooperative driving strategies for nonsignalized intersections, *IEEE Trans. Veh. Technol.*, vol. 67, no. 4, pp. 2900–2911, 2018.
- [11] H. Pei, J. Zhang, Y. Zhang, X. Pei, S. Feng, and L. Li, Fault-tolerant cooperative driving at signal-free intersections, *IEEE Trans. Intell. Veh.*, vol. 8, no. 1, pp. 121–134, 2023.
- [12] H. Xu, Y. Zhang, L. Li, and W. Li, Cooperative driving at unsignalized intersections using tree search, *IEEE Trans. Intell. Transport. Syst.*, vol. 21, no. 11, pp. 4563–4571, 2020.
- [13] H. Xu, C. G. Cassandras, L. Li, and Y. Zhang, Comparison of cooperative driving strategies for CAVs at signal-free intersections, *IEEE Trans. Intell. Transport. Syst.*, vol. 23,

- no. 7, pp. 7614–7627, 2022.
- [14] J. Zhang, H. Pei, X. Ban, and L. Li, Analysis of cooperative driving strategies at road network level with macroscopic fundamental diagram, *Transp. Res. Part C: Emerg. Technol.*, vol. 135, p. 103503, 2022.
- [15] S. Ilgin Guler, M. Menendez, and L. Meier, Using connected vehicle technology to improve the efficiency of intersections, *Transp. Res. Part C: Emerg. Technol.*, vol. 46, pp. 121–131, 2014.
- [16] B. Xu, S. E. Li, Y. Bian, S. Li, X. J. Ban, J. Wang, and K. Li, Distributed conflict-free cooperation for multiple connected vehicles at unsignalized intersections, *Transp. Res. Part C: Emerg. Technol.*, vol. 93, pp. 322–334, 2018.
- [17] H. Xu, Y. Zhang, C. G. Cassandras, L. Li, and S. Feng, A bi-level cooperative driving strategy allowing Lane changes, *Transp. Res. Part C: Emerg. Technol.*, vol. 120, p. 102773, 2020.
- [18] J. Zhang, Z. Li, L. Li, Y. Li, and H. Dong, A bi-level cooperative operation approach for AGV based automated valet parking, *Transp. Res. Part C: Emerg. Technol.*, vol. 128, p. 103140, 2021.
- [19] L. Chen and C. Englund, Cooperative intersection management: A survey, *IEEE Trans. Intell. Transport. Syst.*, vol. 17, no. 2, pp. 570–586, 2016.
- [20] Z. He, L. Zheng, L. Lu, and W. Guan, Erasing lane changes from roads: A design of future road intersections, *IEEE Trans. Intell. Veh.*, vol. 3, no. 2, pp. 173–184, 2018.
- [21] Z. Chen and X. Li, Designing corridor systems with modular autonomous vehicles enabling station-wise docking: Discrete modeling method, *Transp. Res. Part E: Logist. Transp. Rev.*, vol. 152, p. 102388, 2021.
- [22] X. Lin, M. Li, Z. J. M. Shen, Y. Yin, and F. He, Rhythmic control of automated traffic-part II: Grid network rhythm and online routing, *Transp. Sci.*, vol. 55, no. 5, pp. 988–1009, 2021.
- [23] X. Shi and X. Li, Operations design of modular vehicles on an oversaturated corridor with first-in, first-out passenger queueing, *Transp. Sci.*, vol. 55, no. 5, pp. 1187–1205, 2021.
- [24] Q. He, K. L. Head, and J. Ding, PAMSCOD: Platoon-based arterial multi-modal signal control with online data, *Procedia Soc. and Behav. Sci.*, vol. 17, pp. 462–489, 2011.
- [25] X. F. Xie, S. F. Smith, L. Lu, and G. J. Barlow, Schedule-driven intersection control, *Transp. Res. Part C: Emerg. Technol.*, vol. 24, pp. 168–189, 2012.
- [26] H. Liu, X. Y. Lu, and S. E. Shladover, Traffic signal control by leveraging Cooperative Adaptive Cruise Control (CACC) vehicle platooning capabilities, *Transp. Res. Part C: Emerg. Technol.*, vol. 104, pp. 390–407, 2019.
- [27] H. Xu, S. Feng, Y. Zhang, and L. Li, A grouping-based cooperative driving strategy for CAVs merging problems, *IEEE Trans. Veh. Technol.*, vol. 68, no. 6, pp. 6125–6136, 2019.
- [28] G. Lu, Z. Shen, X. Liu, M. Nie, and Z. Xiong, Are autonomous vehicles better off without signals at intersections? A comparative computational study, *Transp. Res. Part B: Methodol.*, vol. 155, pp. 26–46, 2022.
- [29] Q. Ge, Q. Sun, Z. Wang, S. E. Li, Z. Gu, S. Zheng, and L. Liao, Real-time coordination of connected vehicles at intersections using graphical mixed integer optimization, *IET Intell. Trans. Syst.*, vol. 15, no. 6, pp. 795–807, 2021.
- [30] M. W. Levin, S. D. Boyles, and R. Patel, Paradoxes of reservation-based intersection controls in traffic networks, *Transp. Res. Part A: Policy Pract.*, vol. 90, pp. 14–25, 2016.
- [31] M. W. Levin and D. Rey, Conflict-point formulation of intersection control for autonomous vehicles, *Transp. Res. Part C: Emerg. Technol.*, vol. 85, pp. 528–547, 2017.
- [32] Y. Wu, H. Chen, and F. Zhu, DCL-AIM: Decentralized coordination learning of autonomous intersection management for connected and automated vehicles, *Transp. Res. Part C: Emerg. Technol.*, vol. 103, pp. 246–260, 2019.
- [33] E. Lukose, M. W. Levin, and S. D. Boyles, Incorporating insights from signal optimization into reservation-based intersection controls, *J. Intell. Transp. Syst.*, vol. 23, no. 3, pp. 250–264, 2019.
- [34] A. Stevanovic and N. Mitrovic, Combined alternate-direction lane assignment and reservation-based intersection control, in *Proc. 2018 21st Int. Conf. Intelligent Transportation Systems (ITSC)*, Maui, HI, USA, 2018, pp. 14–19.
- [35] R. Tachet, P. Santi, S. Sobolevsky, L. I. Reyes-Castro, E. Frazzoli, D. Helbing, and C. Ratti, Revisiting street intersections using slot-based systems, *PLoS ONE*, vol. 11, no. 3, p. e0149607, 2016.
- [36] S. Li, K. Shu, Y. Zhou, D. Cao, and B. Ran, Cooperative critical turning point-based decision-making and planning for CAVH intersection management system, *IEEE Trans. Intell. Transport. Syst.*, vol. 23, no. 8, pp. 11062–11072, 2022.
- [37] L. Chai, B. Cai, W. Shangguan, J. Wang, and H. Wang, Connected and autonomous vehicles coordinating approach at intersection based on space-time slot, *Transportmetrica A: Transport Science*, vol. 14, no. 10, pp. 929–951, 2018.
- [38] X. Chen, M. Li, X. Lin, Y. Yin, and F. He, Rhythmic control of automated traffic-part I: Concept and properties at isolated intersections, *Transp. Sci.*, vol. 55, no. 5, pp. 969–987, 2021.
- [39] W. Zhao, D. Ngoduy, S. Shepherd, R. Liu, and M. Papageorgiou, A platoon based cooperative eco-driving model for mixed automated and human-driven vehicles at a signalised intersection, *Transp. Res. Part C: Emerg. Technol.*, vol. 95, pp. 802–821, 2018.
- [40] C. Chen, J. Wang, Q. Xu, J. Wang, and K. Li, Mixed platoon control of automated and human-driven vehicles at a signalized intersection: Dynamical analysis and optimal control, *Transp. Res. Part C: Emerg. Technol.*, vol. 127, p. 103138, 2021.
- [41] Y. Yin, Robust optimal traffic signal timing, *Transp. Res. Part B: Methodol.*, vol. 42, no. 10, pp. 911–924, 2008.
- [42] Z. Li, Q. Wu, H. Yu, C. Chen, G. Zhang, Z. Z. Tian, and P. D. Prevedouros, Temporal-spatial dimension extension-based intersection control formulation for connected and autonomous vehicle systems, *Transp. Res. Part C: Emerg. Technol.*, vol. 104, pp. 234–248, 2019.
- [43] C. Yu, W. Ma, and X. Yang, A time-slot based signal scheme model for fixed-time control at isolated intersections, *Transp. Res. Part B: Methodol.*, vol. 140, pp. 176–192, 2020.

- [44] S. E. Shladover, D. Su, and X. Y. Lu, Impacts of cooperative adaptive cruise control on freeway traffic flow, *Transp. Res. Rec.*, vol. 2324, no. 1, pp. 63–70, 2012.
- [45] H. Yu, R. Jiang, Z. He, Z. Zheng, L. Li, R. Liu, and X. Chen, Automated vehicle-involved traffic flow studies: A survey of assumptions, models, speculations, and perspectives, *Transp. Res. Part C: Emerg. Technol.*, vol. 127, p. 103101, 2021.
- [46] V. Milanés, S. E. Shladover, J. Spring, C. Nowakowski, H. Kawazoe, and M. Nakamura, Cooperative adaptive cruise control in real traffic situations, *IEEE Trans. Intell. Transport. Syst.*, vol. 15, no. 1, pp. 296–305, 2014.
- [47] A. Uno, T. Sakaguchi, and S. Tsugawa, A merging control algorithm based on inter-vehicle communication, in *Proc. 199 IEEE/IEEJ/JSAI Int. Conf. Intelligent Transportation Systems*, Tokyo, Japan, 1999, pp. 783–787.
- [48] T. Sakaguchi, A. Uno, S. Kato, and S. Tsugawa, Cooperative driving of automated vehicles with inter-vehicle communications, in *Proc. IEEE Intelligent Vehicles Symp. 2000*, Dearborn, MI, USA, 2000, pp. 516–521.
- [49] L. Zhang and D. Levinson, Balancing efficiency and equity of ramp meters, *J. Transp. Eng.*, vol. 131, no. 6, pp. 477–481, 2005.
- [50] L. Zhang and D. Levinson, Ramp metering and freeway bottleneck capacity, *Transp. Res. Part A: Policy Pract.*, vol. 44, no. 4, pp. 218–235, 2010.
- [51] Q. Tian, H. J. Huang, H. Yang, and Z. Gao, Efficiency and equity of ramp control and capacity allocation mechanisms in a freeway corridor, *Procedia Soc. Behav. Sci.*, vol. 17, pp. 509–531, 2011.
- [52] X. Liang, S. I. Guler, and V. V. Gayah, An equitable traffic signal control scheme at isolated signalized intersections using connected vehicle technology, *Transp. Res. Part C: Emerg. Technol.*, vol. 110, pp. 81–97, 2020.
- [53] H. Pei, S. Feng, Y. Zhang, and D. Yao, A cooperative driving strategy for merging at on-ramps based on dynamic programming, *IEEE Trans. Veh. Technol.*, vol. 68, no. 12, pp. 11646–11656, 2019.
- [54] J. Ding, H. Peng, Y. Zhang, and L. Li, Penetration effect of connected and automated vehicles on cooperative on-ramp merging, *IET Intell. Transp. Syst.*, vol. 14, no. 1, pp. 56–64, 2020.
- [55] S. Feng, Z. Song, Z. Li, Y. Zhang, and L. Li, Robust platoon control in mixed traffic flow based on tube model predictive control, *IEEE Trans. Intell. Veh.*, vol. 6, no. 4, pp. 711–722, 2021.
- [56] J. Ge, H. Xu, J. Zhang, Y. Zhang, D. Yao, and L. Li, Heterogeneous driver modeling and corner scenarios sampling for automated vehicles testing, *J. Adv. Transp.*, vol. 2022, p. 8655514, 2022.
- [57] J. Zhang, S. Li, and L. Li, Coordinating CAV swarms at intersections with a deep learning model, *IEEE Trans. Intell. Transport. Syst.*, doi: 10.1109/TITS.2023.3250704.



Shen Li received the PhD degree from the University of Wisconsin-Madison, USA in 2018. He is currently a research associate at Tsinghua University, China. His research interests include intelligent transportation systems, CAVH system architecture design, vehicle-infrastructure cooperative planning and decision methods, traffic data mining

based on cellular data, and traffic operations and management.



Jiawei Zhang received the BEng from Tsinghua University, China in 2020. He is currently a PhD candidate at the Department of Automation, Tsinghua University, Beijing, China. His research interests include intelligent transportation systems, Connected and Automated Vehicles (CAVs), and deep reinforcement

learning.



Zhenwu Chen received the BEng and MEng degrees from Tongji University, China in 2006 and 2009, respectively. He is currently working at the Shenzhen Urban Transport Planning Center Co., Ltd., China. His research interests include intelligent transportation system, traffic control, and autonomous driving.



Li Li received the PhD degree from the University of Arizona, USA in 2005. He is currently a professor at the Department of Automation, Tsinghua University, Beijing, China. His research interests include artificial intelligence, intelligent control and sensing, intelligent transportation systems, and intelligent vehicles. He has published

over 150 SCI-indexed international journal articles and over 70 international conference papers as the first/corresponding author. He is a member of the editorial advisory board for *Transportation Research Part C: Emerging Technologies*, and a member of the editorial board for *Transport Reviews* and *Acta Automatica Sinica*. He also serves as an associate editor for *IEEE Transactions on Intelligent Transportation Systems* and *IEEE Transactions on Intelligent Vehicles*.